BMC Medical Imaging

RESEARCH

Open Access

Alterations of gray matter volume and structural covariance network in unilateral frontal lobe low-grade gliomas

Yue Hu[1†], Jianxun Xu[2†], Ji Xiong[3], Kun Lv[1*] and Daoying Geng[1*]

Abstract

Purpose To explore the alterations of gray matter volume (GMV) and structural covariant network (SCN) in unilateral frontal lobe low-grade gliomas (FLGGs).

Materials and methods The three dimensional (3D) T1 structural images of 117 patients with unilateral FLGGs and 68 age- and sex-matched healthy controls (HCs) were enrolled. The voxel-based morphometry (VBM) analysis and graph theoretical analysis of SCN were conducted to investigate the impact of unilateral FLGGs on the brain structure. This represents the first structural MRI study integrating both voxel-level morphometric changes and network-level reorganization patterns in unilateral FLGGs.

Results Through VBM analysis, we found that unilateral FLGGs can cause increased GMV in contralesional amygdala, calcarine, and angular gyrus, ipsilesional amygdala as well as vermis_6. The SCN of contralesional cerebrum, ipsilesional unaffected regions and cerebellum in both patients and HCs have typical small-world properties (Sigma > 1, Lambda ≈ 1 and Gamma > 1). Compared to HCs, global and nodal network metrics changed significantly in patients.

Conclusion The combination of VBM and SCN analysis revealed both focal GMV enlargement and topological alterations in patients with unilateral FLGGs, and provide a novel perspective of cross regional morphological collaborative changes for understanding the glioma-related neuroadaptation. These findings may suggest potential neuroimaging correlates of adaptive changes, which could inform future investigations into personalized treatment approaches.

Clinical trial number Not applicable.

Keywords Frontal lobe, Low-grade gliomas, Gray matter volume, Graph theoretical analysis, Structural covariance network

[†]Yue Hu and Jianxun Xu contributed equally to this work.

*Correspondence:
Kun Lv
klv20@fudan.edu.cn
Daoying Geng
gdy_2019@163.com

[1]Department of Radiology, Huashan Hospital, Fudan University, 12 Wulumuqi Middle Road, Shanghai 200040, P. R. China
[2]Nantong University, Jiangsu, China
[3]Department of Pathology, Huashan Hospital, Fudan University, Shanghai, China

© The Author(s) 2025. **Open Access** This article is licensed under a Creative Commons Attribution-NonCommercial-NoDerivatives 4.0 International License, which permits any non-commercial use, sharing, distribution and reproduction in any medium or format, as long as you give appropriate credit to the original author(s) and the source, provide a link to the Creative Commons licence, and indicate if you modified the licensed material. You do not have permission under this licence to share adapted material derived from this article or parts of it. The images or other third party material in this article are included in the article's Creative Commons licence, unless indicated otherwise in a credit line to the material. If material is not included in the article's Creative Commons licence and your intended use is not permitted by statutory regulation or exceeds the permitted use, you will need to obtain permission directly from the copyright holder. To view a copy of this licence, visit http://creativecommons.org/licenses/by-nc-nd/4.0/.

Introduction

Glioma is considered to be the most prevalent primary malignancy of central nervous system (CNS), with a marked tendency to invade the frontal lobe [1]. Lesions in the frontal lobe commonly result in language and cognitive dysfunction, greatly diminishing the patient's quality of life. Fortunately, numerous studies have consistently highlighted the remarkable capacity of brain for functional and structural reorganization in response to intrinsic and extrinsic stimuli. This property, known as neuroadaptation, occurs across the lifespan, both physiological development and novel learning [2, 3], and also serves as an adaptive mechanism supporting functional recovery after brain injury [4, 5]. Notably, neuroadaptation in glioma exhibits a hierarchical pattern [6], wherein reorganization progresses from local perilesional adaptation to recruitment of contralesional homologs and higher-order networks. This pattern is particularly suited for low-grade gliomas (LGGs), given their indolent growth, prolonged timeline for adaptive rewiring, and minimal disruption of neuronal migration [7].

The elucidation of functional and structural reorganization patterns in brain tumors has long been a fundamental pursuit in clinical neuro-oncology. This line of inquiry carries profound clinical implications, as it not only advances the comprehension of mechanisms pertinent to disease progression and prognosis but also furnishes fresh perspectives on novel and more effective treatment interventions. Functional imaging studies have revealed that compensatory activity was initially observed in perilesional tissue (residual neurons adjacent to tumors) and subsequently extends to distal networks [8, 9]. Nevertheless, the extent to which these functional reorganization are accompanied by alterations in macrostructure remains an unresolved question.

Although several works have investigated the alterations of gray matter volume (GMV) in gliomas by voxel-based morphometry (VBM) [7, 10, 11], morphological analysis alone is inadequate to fully dissect the mechanisms driving brain structural reorganization. It is well-established that neuroplasticity in gliomas involves not only local morphological changes but also large-scale network adaptations to preserve function [6, 8]. Structural covariance network (SCN), which quantify network-level covariance patterns in morphological properties, provide a unique lens to study these network-level reorganizations. Unlike functional or diffusion-based networks, SCN reflect synchronized developmental, pathological, or compensatory changes in morphometry over time, likely driven by shared genetic, neurotrophic, or activity-dependent mechanisms [12]. Utilizing the SCN, multiple investigations have mapped focal and whole-brain correlations of morphological properties including GMV, surface area, and cortical thickness in healthy subjects and neurodegenerative diseases like mild cognitive impairment, Parkinson's disease, Alzheimers disease and so on [13–15]. While previous studies have mapped structural covariance patterns in neurodegenerative disorders, critical gaps persist in glioma research: (1) lack of network-level characterization of GM reorganization, (2) inadequate attention to cerebellar contributions. Therefore, the present study aimed to examine the changes of GMV and topological alterations of SCN in unilateral frontal lobe low-grade gliomas (FLGGs).

Materials and methods

Participants

This retrospective study of gliomas, treated at our hospital from 2019 to 2023, was granted approval by the institutional review board. Written informed consent were obtained from all subjects in this study. The inclusion criteria: (1) pathologically confirmed unilateral FLGGs with isocitrate dehydrogenase (IDH)-mutant (WHO grade 2, according to 2021 WHO classification system [16]), (2) right-handedness and 18–70 years old, and (3) solitary mass. The exclusion criteria: (1) high-grade gliomas (HGGs) (WHO grade 3/4), (2) patients who had undergone treatment including surgery, biopsy, radiotherapy, or pharmacological therapy before the magnetic resonance imaging (MRI) scans, (3) patients with other intracranial abnormalities, (4) midline shift and bilateral hemispheres involved, and (5) MRI acquisition issues, such as artifacts. Healthy controls (HCs) comprising right-handed, age- and sex-matched healthy volunteers devoid of organic, mental, or psychological disorders were also recruited.

MRI

All participants underwent 3T MRI (Siemens Viero MR, Erlangen, Germany) scans with an 8-channel head coil within a week prior to treatment. The scanning protocol included three dimensional (3D) structural T1 and T2-weighted fluid attenuation inversion recovery (FLAIR). The main parameters of 3D T1 were: repetition time (TR) = 1900ms; echo time (TE) = 2.93ms; slice thickness = 1 mm; field of view (FOV) = 256 mm×256 mm; flip angle = 12°; matrix = 256 × 256. The main parameters of T2-weighted FLAIR were: TR = 8000ms; TE = 102ms; FOV = 201 mm×230 mm; matrix = 256 × 190; thickness = 6 mm.

Tumor masking

To visualize the lesion and calculate tumor volume (TV), an experienced neuroradiologist with 6 years of expertise delineated the tumor mask on T2-weighted FLAIR images using MRIcron (https://www.mccauslandcenter.sc.edu/crnl/tools) and reconfirmed by a senior neuroradiologist (DY.G, 30 years of experience). The tumor mask

included tumor-affected zones appearing hyperintense on T2-weighted FLAIR. Rechecked lesion masks and T2-weighted images were normalized to standard Montreal Neurological Institute (MNI) space and then all normalized lesion masks were superimposed to generate lesion overlap by SPM12 (https://www.fil.ion.ucl.ac.uk/spm/software/spm12/). The lesion overlap was visualized with MRIcroGL (https://www.mccauslandcenter.sc.edu/mricrogl)(Fig. 1).

Image preprocessing

The preprocessing of 3D T1 images was performed on SPM12 and CAT12 toolbox in MATLAB (release 2022a, MathWorks, Inc., Natick, MA). Due to the limited number of right FLGGs, images of right-sided lesions were flipped along the mid-sagittal line before preprocessing to enhance statistical power. However, this operation could introduce bias due to the asymmetry between left and right hemispheres. In order to weaken this bias, we conducted comparative analysis of age, sex, TV, and total intracranial volume (TIV) between the patients with right- and left-sided lesions. We further performed Levene's test for homogeneity of variance between left and right FLGG subgroups, confirming equal variances across compared parameters. As we found no significant differences, we flipped right-sided lesions in our study. Images were manually reoriented, with the anterior commissure designated as the origin (coordinates: 0, 0, 0), and then were segmented into GM, white matter (WM), and cerebrospinal fuid (CSF). The 3D T1 structural images were normalized to standard MNI space with an isotropic voxel resolution of $1.5 \times 1.5 \times 1.5 mm^3$, and then

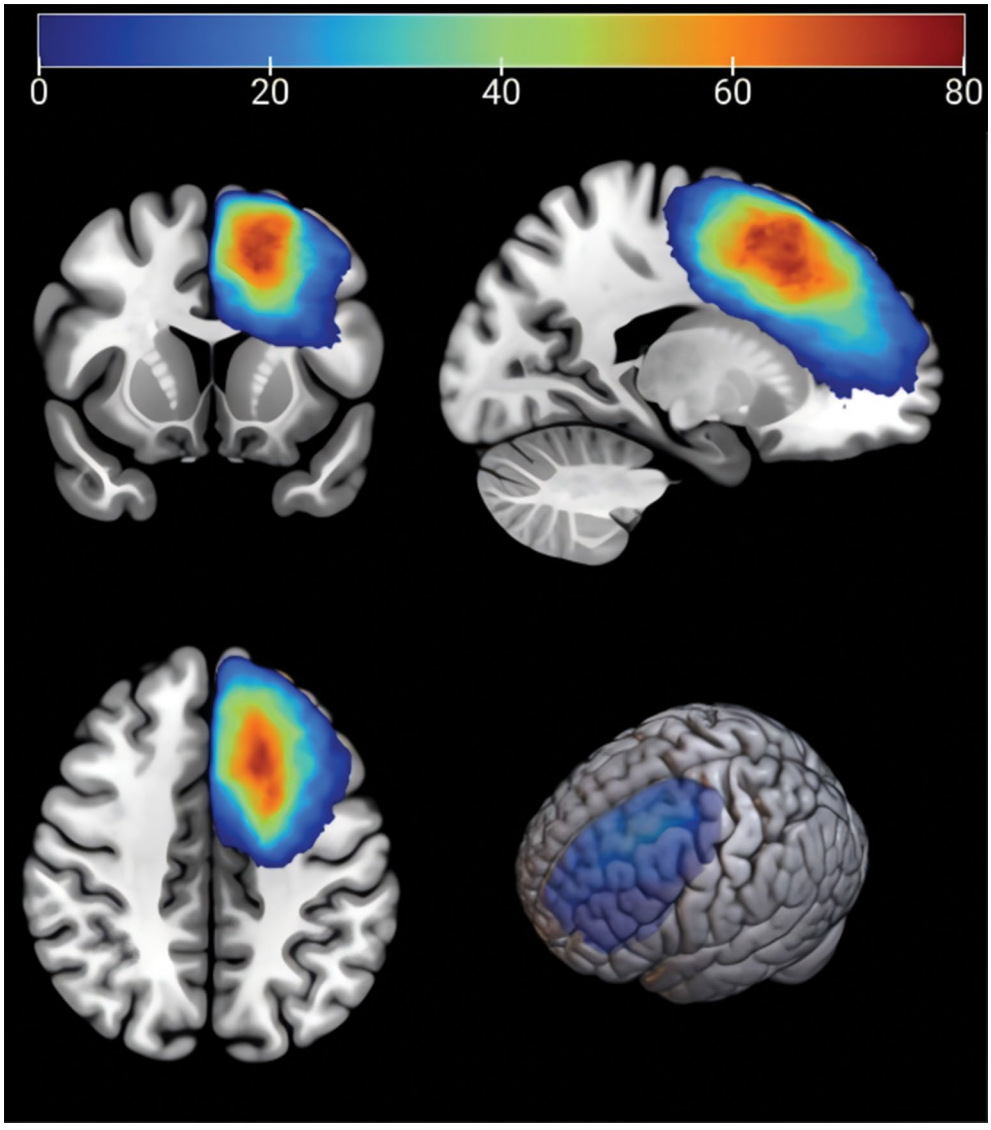

Fig. 1 Lesion overlap

were modulated to maintain original GMV. Meanwhile, the TIV were extracted for all subjects. The modulated GM maps were smoothed with an 8 mm full width at half-maximum Gaussian kernel. Subjects with weighted image quality rating (IQR) < 85% were excluded.

VBM

After preprocessing, we assessed the difference in GMV between the patients and HCs using two sample t-test in CAT12 with TIV, age and sex as covariates. We applied absolute masking with a 0.2 threshold and proportional scaling for global normalization according to a prior study [10]. Region-specific masks were generated in the WFU-Pickatlas toolbox (https://www.nitrc.org/projects/wfu_pickatlas/) for observing the changes of contralesional cerebrum, ipsilesional unaffected regions and cerebellum. The family wise error (FWE) was used for correction with $p < 0.05$ at the cluster level and k > 200 of cluster sizes.

SCN

SCN analysis was conducted on the GRETNA toolbox in MATLAB through the following protocol: (1) contralesional cerebrum, ipsilesional unaffected regions and cerebellum were divided into different regions with the automated anatomical labeling (AAL) atlas segmentation scheme, and GMV was determined for each region. (2) TIV, age and sex were classified as covariates. Pearson correlation coefficients were then calculated for the GMV between brain regions, culminating in a correlation matrix (Fig. 2). (3) a sparsity range (0.05–0.5, step size = 0.01) was established for the correlation matrix to ensure complete connectivity and small-world properties within the brain network. (4) based on this sparsity range, the correlation matrix was converted into a binary matrix, which was utilized to compute graph metrics. The global metrics included small-world properties (normalized clustering coefficient (Gamma), normalized characteristic path length (Lambda), and small-world-ness (Sigma)), integration metrics (global efficiency (Eg) and characteristic path length (Lp)), and segregation metrics (local efficiency (Eloc) and clustering coefficient (Cp)). The nodal metrics included betweenness centrality (BC), degree centrality (DC), and nodal efficiency (NE). The differences of these network metrics were determined with permutation test (1000 times). The false discovery rate (FDR) was used for nodal metrics with $p < 0.05$.

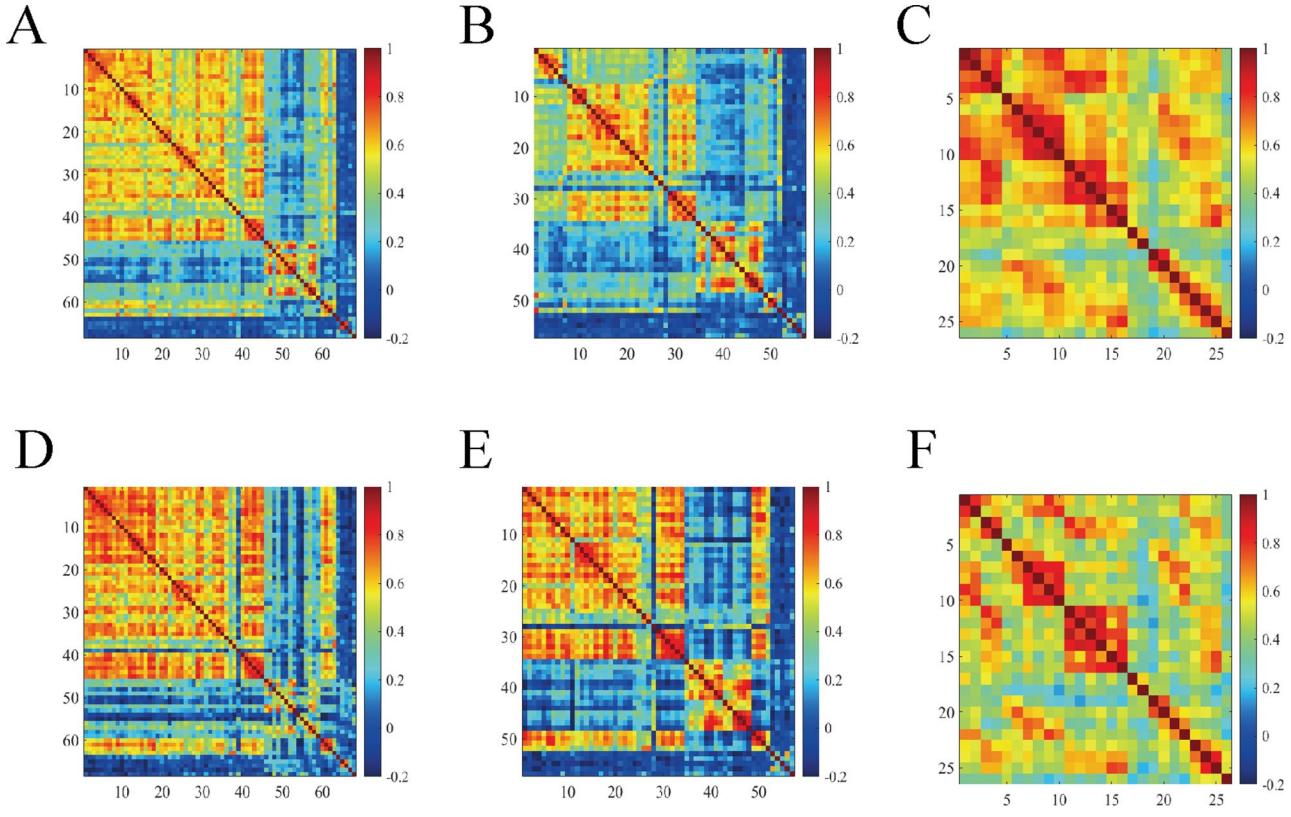

Fig. 2 Correlation matrices. **A** and **D**: Correlation matrices of contralesional cerebrum for the unilateral FLGGs (**A**) and the HCs (**D**). **B** and **E**: Correlation matrices of ipsilesional unaffected regions for the unilateral FLGGs (**B**) and the HCs (**E**). **C** and **F**: Correlation matrices of cerebellum for the unilateral FLGGs (**C**) and the HCs (**F**). FLGGs frontal lobe low-grade gliomas, HCs healthy controls

Statistical analysis

Quantitative variables (age, TV, and TIV) were compared using two sample t test, and sex was compared using chi-square test. Statistical analysis were performed on Statistical Package for Social Sciences software (SPSS 26.0 SPSS Inc., Chicago, IL, USA, 1999). Quantitative variables are reported as mean ± standard deviation. Statistical significance was set at $p < 0.05$.

Results

Participants demographics

Our study enrolled 117 patients with unilateral FLGGs (98 patients with left FLGGs, 19 patients with right FLGGs) and 68 age-and sex-matched HCs. Demographic characteristics were summarized in Table 1. Statistical tests revealed no significant differences in age, sex, TIV, or TV between patients and HCs, nor between patients with right- and left-sided lesions.

VBM

Patients with unilateral FLGGs exhibited significantly larger GMV in contralesional amygdala, calcarine, and angular gyrus, ipsilesional amygdala as well as vermis_6 compared to HCs (Fig. 3). The surviving clusters include 22,122 voxels (x = 21, y = 1.5, z = − 18 with T = 11.17) in contralesional amygdala, 1543 voxels (x = 12, y = − 96, z = 0 with T = 6.62) in contralesional calcarine, 513 voxels (x = 52.5, y = − 58.5, z = 31.5 with T = 5.54) in contralesional angular gyrus, 35,475 voxels (x = − 19.5, y = − 3, z = − 16.5 with T = 12.65) in ipsilesional amygdala, and 22,972 voxels (x = 3, y = − 67.5, z = − 18 with T = 10.04) in vermis_6 (Table 2).

SCN

Topological alterations of the contralesional cerebrum

Global network metrics The SCN of contralesional cerebrum in both patients and HCs demonstrated typical small-world properties (Sigma > 1, Lambda ≈ 1 and Gamma > 1). Patients showed significantly increased Sigma, Gamma, Cp, Eloc, Eg, and decreased Lp compared to HCs. Lambda did not differ significantly between groups (Fig. 4).

Nodal network metrics Patients exhibited significantly decreased BC in contralesional opercular part of inferior frontal gyrus and orbital part of medial frontal gyrus, with significantly increased BC in other contralesional regions such as orbital part of inferior frontal gyrus, medial part of superior frontal gyrus, hippocampus, postcentral gyrus, and angular gyrus compared to HCs. Similarly, the DC of contralesional opercular part of inferior frontal gyrus was significantly decreased in patients, while DC of contralesional orbital part of inferior frontal gyrus, hippocampus, postcentral gyrus and angular gyrus were significantly increased. The NE of contralesional opercular part of inferior frontal gyrus and orbital part of medial frontal gyrus were significantly decreased in patients, while NE of contralesional orbital part of inferior frontal gyrus, medial part of superior frontal gyrus, hippocampus, postcentral gyrus, supramarginal gyrus and heschl gyrus were significantly increased (Fig. 5).

Topological alterations of the ipsilesional unaffected regions

Global network metrics The SCN of ipsilesional unaffected regions in both patients and HCs demonstrated typical small-world properties (Sigma > 1, Lambda ≈ 1 and Gamma > 1). Patients showed significantly increased Sigma, Eg, and decreased Lp, Lambda, Eloc, and Cp compared to HCs. Gamma did not differ significantly between groups (Fig. 6).

Nodal network metrics Patients exhibited significantly decreased BC in ipsilesional cuneus, postcentral gyrus and angular gyrus, significantly decreased DC in ipsilesional postcentral gyrus, angular gyrus and heschl gyrus as well as significantly decreased NE in ipsilesional cuneus, angular gyrus, heschl gyrus and superior temporal gyrus compared to HCs (Fig. 7).

Table 1 Demographic characteristics

Variables	Unilateral FLGGs	HCs	*P* values	Left FLGGs	Right FLGGs	*P* values
No	117	68	NA	98	19	NA
Age, years	38.11 ± 9.69	39.47 ± 5.49	0.225	37.98 ± 9.83	38.79 ± 9.14	0.740
Sex ratio, F/M, n	60/57	33/35	0.718	49/49	11/8	0.529
TIV, cm^3	1450.90 ± 141.04	1463.00 ± 153.79	0.587	1457.80 ± 139.78	1415.10 ± 145.91	0.229
TV, cm^3	44.77 ± 37.03	NA	NA	44.58 ± 37.69	45.77 ± 35.44	0.900

Quantitative variables are expressed as the mean ± standard deviation. The *P* values were determined by two-sample t test for age, TIV, and TV, chi-square test for sex ratio

F female, FLGGs frontal low-grade gliomas, HCs healthy controls, M male, NA not applicable, TIV total intracranial volume, TV tumor volume

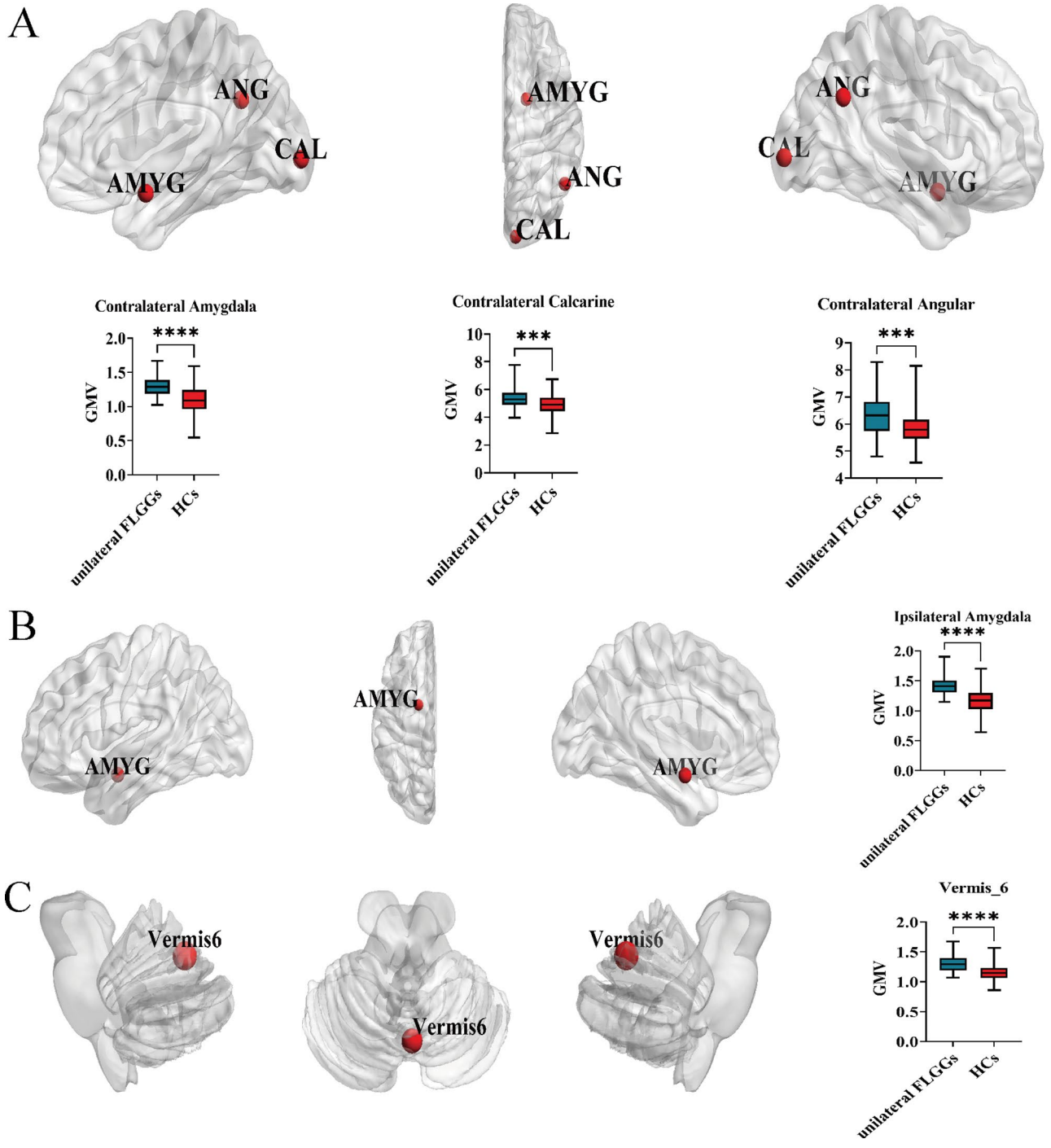

Fig. 3 The GMV of patients with unilateral FLGGs compared with HCs. Patients with unilateral FLGGs exhibited significantly larger GMV in contralesional amygdala, calcarine, and angular gyrus (**A**), ipsilesional amygdala (**B**) as well as vermis_6 (**C**) compared to HCs. AMYG amygdala, ANG angular gyrus, CAL calcarine, FLGGs frontal lobe low-grade gliomas, GMV gray matter volume, HCs healthy controls

Topological alterations of the cerebellum

Global network metrics The SCN of cerebellum in both patients and HCs demonstrated typical small-world properties (Sigma > 1, Lambda ≈ 1 and Gamma > 1). Patients showed significantly decreased Sigma, Gamma, Cp and Eloc compared to HCs. Eg, Lp and Lambda did not differ significantly between groups (Fig. 8).

Nodal network metrics There was no significant difference in nodal metrics of the cerebellum network between patients and HCs.

Table 2 VBM analyses for patients with unilateral FLGGs compared with HCs

ROI	Contract	Brain region	Peak MNI coordinate			Cluster size (in voxels)	Peak level *t* value	*P* values
			X	*Y*	*Z*			
Contralesional cerebrum	Unilateral FLGGs > HCs	Amygdala	21	1.5	-18	22,122	11.17	0.000
		Calcarine	12	-96	0	1543	6.62	0.000
		Angular	52.5	-58.5	31.5	513	5.54	0.000
Ipsilesional unaffected regions		Amygdala	-19.5	-3	-16.5	35,475	12.65	0.000
Cerebellum		Vermis_6	3	-67.5	-18	22,972	10.04	0.000

Clusters survived at a threshold of $P < 0.05$ with family-wise error correction (FWE)

FLGGs frontal low-grade gliomas, HCs healthy controls, MNI Montreal Neurological Institute, ROI region of interest, VBM voxel-based morphometry

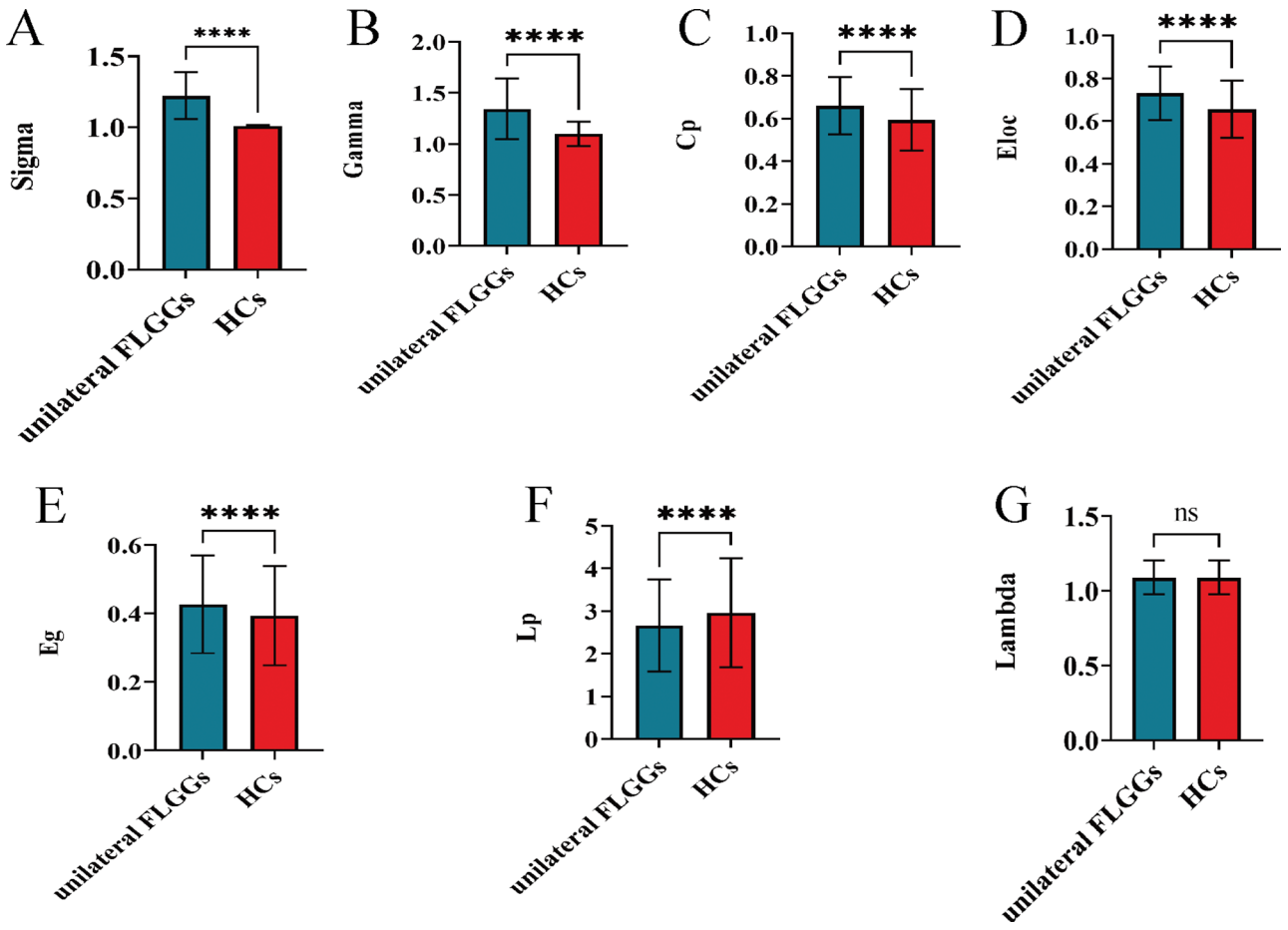

Fig. 4 Alterations in global network metrics of the contralesional cerebrum. Patients with unilateral FLGGs showed significantly increased Sigma (**A**), Gamma (**B**), Cp (**C**), Eloc(**D**), Eg (**E**) and decreased Lp (**F**) compared to HCs. Lambda (**G**) did not differ significantly between groups. Sigma, small-worldness; Gamma, normalized clustering coefficient; Lambda, normalized characteristic path length; Eg, global efficiency; Lp, characteristic path length; Eloc, local efficiency; Cp, clustering coefficient. FLGGs frontal lobe low-grade gliomas, HCs healthy controls

Discussion

Through VBM analysis, we observed that unilateral FLGGs can lead to increased GMV in contralesional amygdala, calcarine, angular gyrus, and ipsilesional amygdal, consistent with potential neuroadaptive processes in the contralateral and ipsilateral hemispheres. While our VBM analysis did not detect GMV increases in contralesional homotopic regions, this null finding may reflect methodological and neurobiological factors. First, stringent cluster-level correction (FWE $p < 0.05$, $k > 200$) prioritized specificity over sensitivity, potentially obscuring subtle GMV changes. Second, frontal LGGs may induce compensatory shifts toward multimodal hubs (e.g., angular gyrus) rather than homotopic prefrontal regions, as evidenced by SCN-derived nodal metrics alterations. The amygdala, with widespread connections

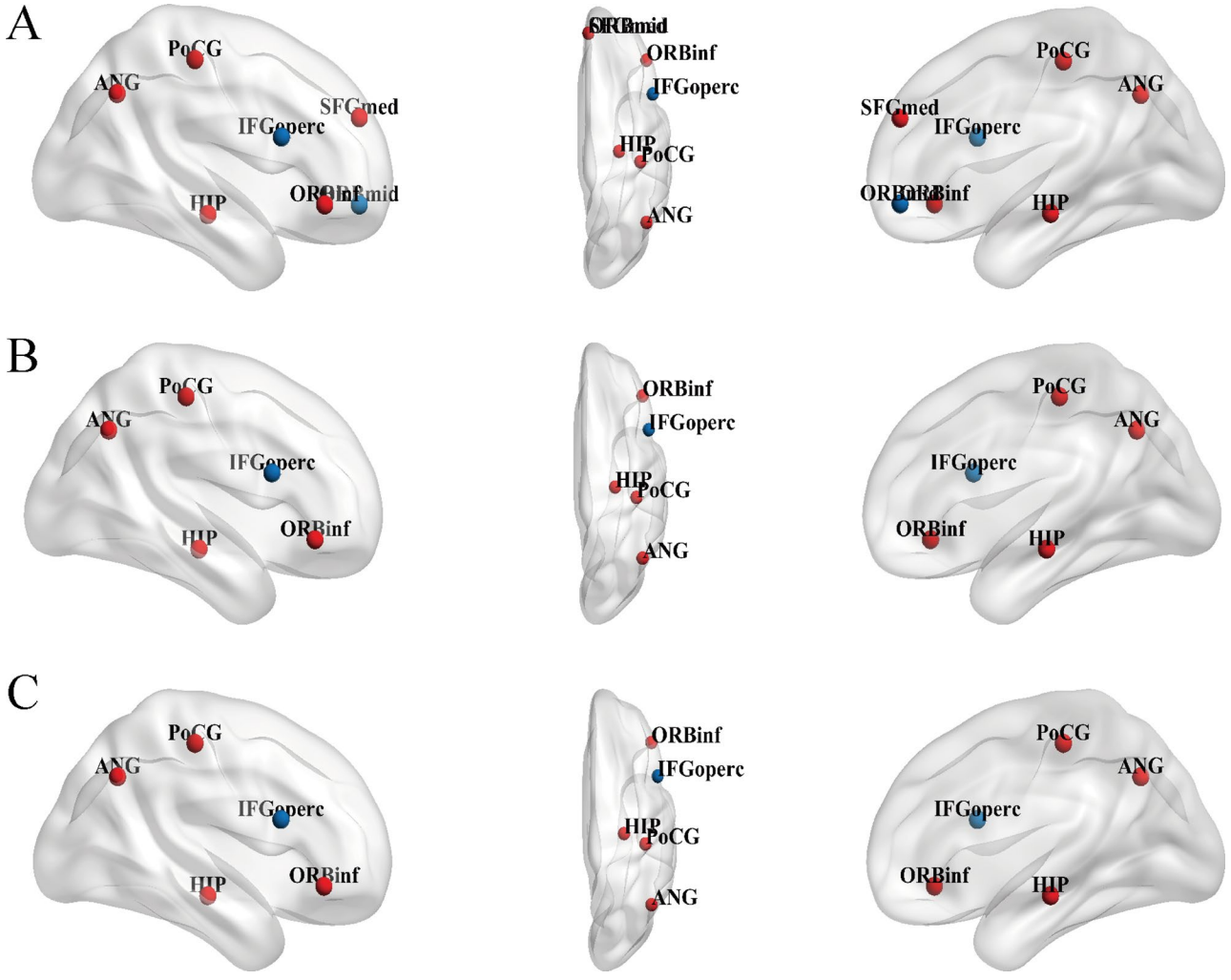

Fig. 5 Alterations in nodal network metrics of the contralesional cerebrum. Comparison of the alterations of nodal network metrics in patients with unilateral FLGGs and HCs including BC (**A**), DC (**B**) and NE (**C**). The red and blue balls represent increased and decreased of the corresponding nodal network metrics respectively. BC, betweenness centrality; DC, degree centrality; NE, nodal efficiency. FLGGs frontal lobe low-grade gliomas, HCs healthy controls

to cortical and subcortical structures, is pivotal in multimodal information processing, emotion recognition, and behavioral modulation [17]. The occipital cortex is the primary brain region of the visual cortex, and the calcarine, as an important component of the occipital cortex, plays a central role in visual processing and bottom-up attentional control [18, 19]. The angular gyrus, situated at the junction of the temporal, occipital, and parietal lobes, possesses extensive white matter fiber bundle connections, suggesting its role in cross-regional information integration. Based on numerous researches in brain injury and neuroimaging, angular gyrus is considered as a vital brain region for semantic processing [20–22]. Given the significance of the amygdala, calcarine, and angular gyrus in brain function, it is plausible that their enlargement of GMV may facilitate compensation to better fulfill function in patients. Our finding of increased contralesional amygdala was consistent with that of Lv et al. [10]. Additionally, compare to Lv et al. [10], we also found that the GMV of ipsilesional amygdala in patients was signifcantly larger than that of HCs by exploring the ipsilesional unaffected regions. Previous studies have reported diverse findings. Xu et al. [23]observed increased GMV in the contralesional cuneus and ipsilateral thalamus of glioma patients, Liu et al. [24]found increased GMV in the left superior parietal gyrus within the cognitive control network in patients with right frontal tumors and Zhang et al. [25] reported widespread GM atrophy in regions such as the temporal lobe, precuneus, lingual gyrus, fusiform, and insula in patients with frontal gliomas. The heterogeneity of participants, the complex and dynamic nature of brain plasticity and the relatively small sample of these studies may account for the discrepancies observed with our findings.

To our knowledge, the majority of existing research on structural and functional reorganization in brain injury

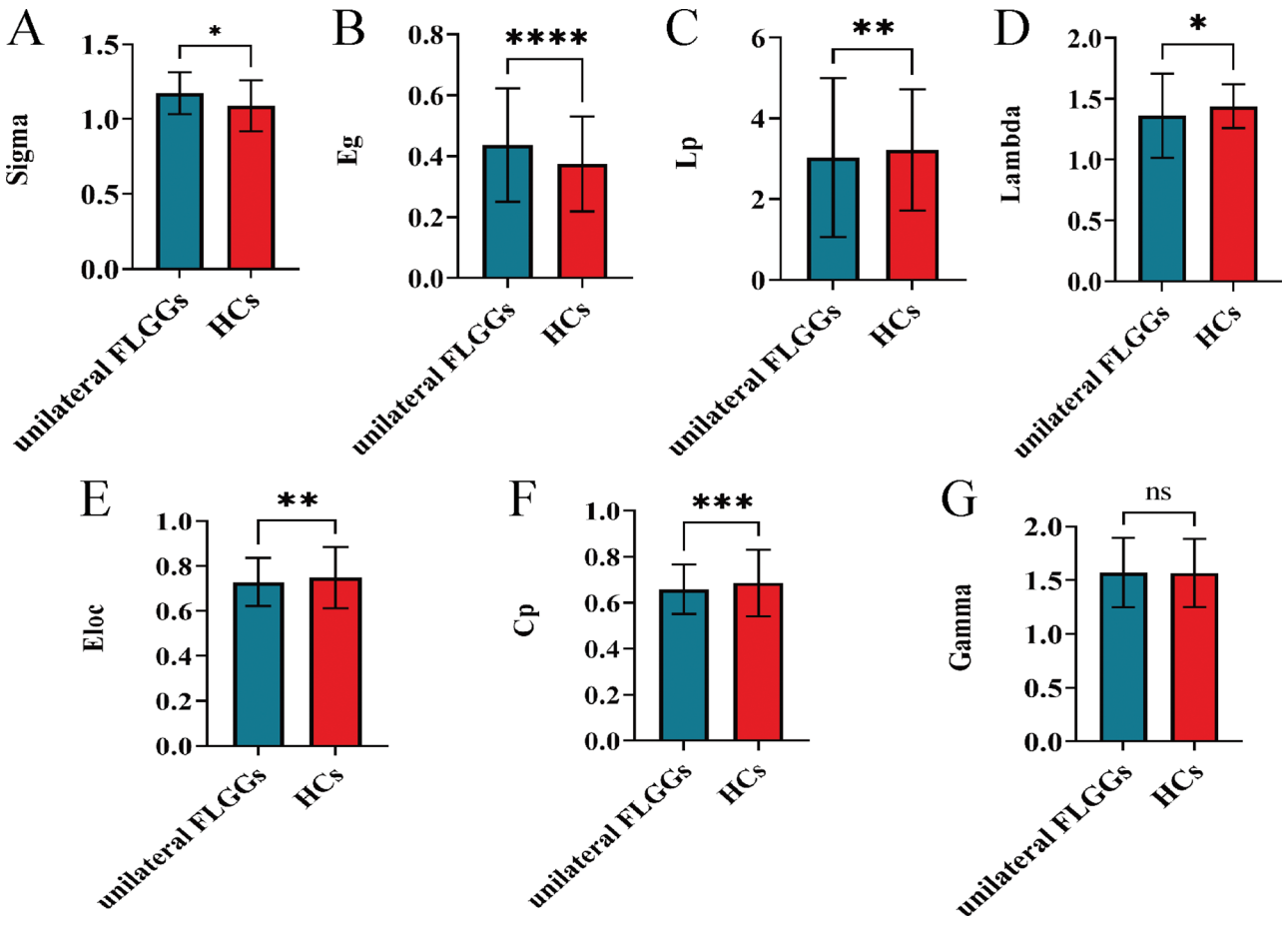

Fig. 6 Alterations in global network metrics of the ipsilesional unaffected regions. Patients with unilateral FLGGs showed significantly increased Sigma (**A**), Eg (**B**) and decreased Lp (**C**), Lambda (**D**), Eloc (**E**) and Cp (**F**) compared to HCs. Gamma (**G**) did not differ significantly between groups. Sigma, small-world-ness; Gamma, normalized clustering coefficient; Lambda, normalized characteristic path length; Eg, global efficiency; Lp, characteristic path length; Eloc, local efficiency; Cp, clustering coefficient. FLGGs frontal lobe low-grade gliomas, HCs healthy controls

has primarily targeted the cerebral cortex, while the cerebellar role in this context, particularly among glioma patients, has received insufficient attention. Traditionally, it was believed that the cerebellum primarily participates in regulating bodily balance, muscle tone, and coordinating voluntary movements. However, recent advancements in research have elucidated the engagement of cerebellum in various cognitive processes such as memory, work, learning, and language [26–28]. In the context of pathological conditions, its role has also garnered attention. For example, patients with cerebellar lesions showed memory impairments similar to those in patients with frontal lesions [29]. Moreover, studies on cerebellar lesions in children further substantiated the cerebellum's involvement in visual-spatial working memory [30]. In our study, unilateral FLGGs patients exhibited greater GMV in vermis_6, indicating the reorganization of cerebellar structure in glioma patients. We hypothesize a cortico-cerebello-thalamo-cortical loop adaptation, where increased cerebellar GMV compensates for disrupted cerebral cortex. Similar to our finding, a prior study observed that patients with left hemispheric LGG had larger GMV in the medial part of bilateral cerebellar lobule VIIa than HCs. In addition, this prior study also found that LGG patients exhibited increased brain activity in regions of cerebellum with greater GMV, suggesting a structure-function coupled alteration [31].

Our investigation also demonstrated that patients with unilateral FLGGs maintained typical small-world properties, yet showed alterations in global and nodal network metrics by graph theoretical analysis based on SCN. Prior researches have documented the small-world properties of resting-state functional and WM structural brain networks in glioma patients [32–34]. Our study further confirmed that the GMV-based SCN of unilateral FLGGs patients also displays small-world properties, suggesting preserved capacity for information processing despite structural alterations. Eloc and Cp serve as assessments of local connectivity and clustering within the brain network, while Eg functions as an indicator of global connectivity. Lp reflects the minimal cost for a network node to transmit information to

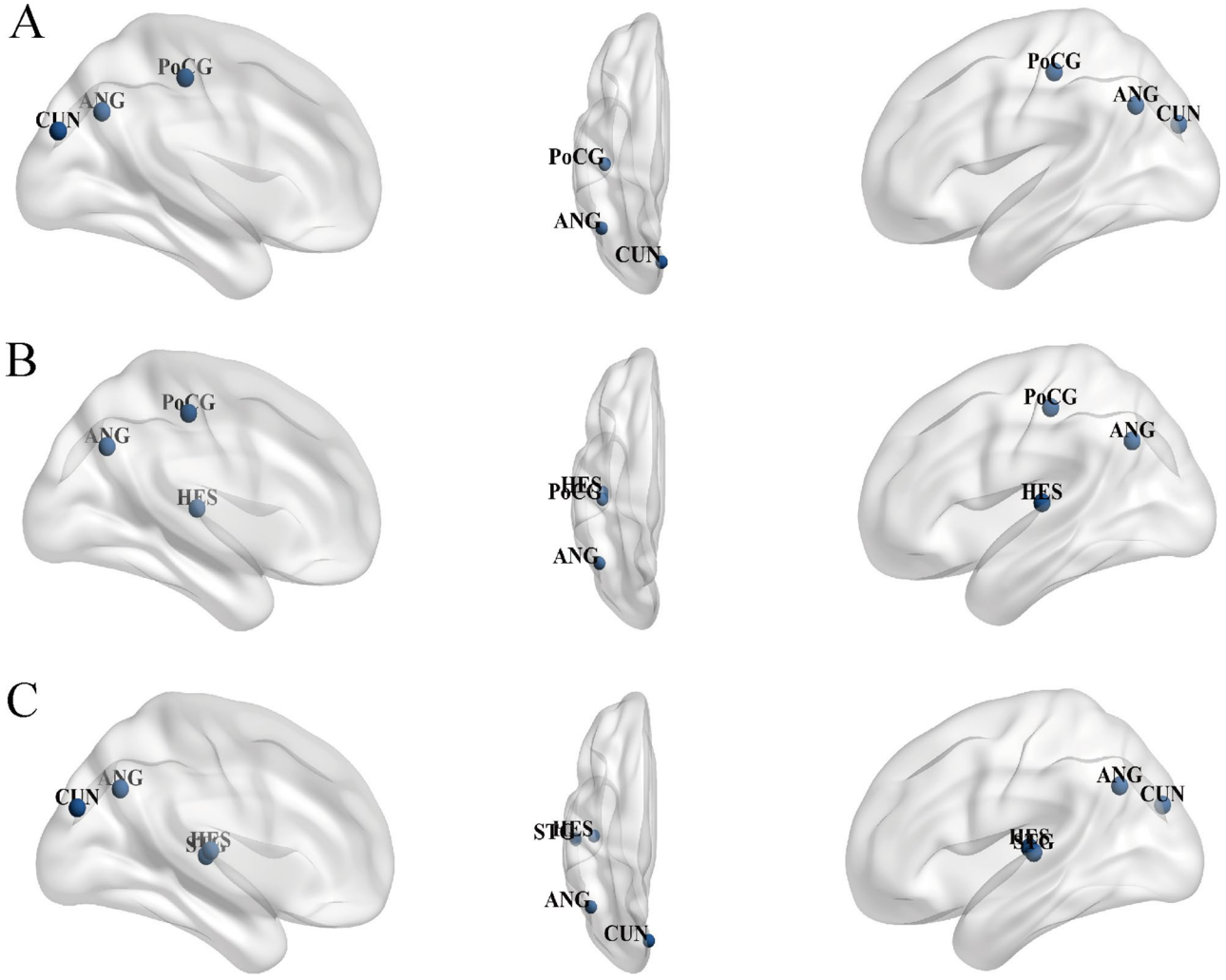

Fig. 7 Alterations in nodal network metrics of the ipsilesional unaffected regions. Comparison of the alterations of nodal network metrics in patients with unilateral FLGGs and HCs including BC (**A**), DC (**B**) and NE (**C**). The blue balls represent decreased of the corresponding nodal network metrics. BC, betweenness centrality; DC, degree centrality; NE, nodal efficiency. FLGGs frontal lobe low-grade gliomas, HCs healthy controls

other nodes. Our results indicated the alterations of SCN in the contralesional cerebrum (increased Eloc, Cp, Eg and decreased Lp) and the ipsilesional unaffected regions (increased Eg and decreased Eloc, Cp, Lp) in unilateral FLGGs patients. The observed increases in Cp and Eloc in the contralesional cerebrum may indicate altered local connectivity patterns, potentially reflecting adaptive reorganization mechanisms. Conversely, the decreased Cp and Eloc in ipsilesional unaffected regions may indicate disorganization of local clustering due to tumor infiltration or diaschisis. Notably, the separation decreased, while integration remained relatively stable in the cerebellum in patients. These findings collectively suggest that glioma-induced structural alterations were hierarchical: (1) decentralization of ipsilesional regions to reduce reliance on compromised nodes; (2) compensation in contralesional hubs and (3) preservation of global efficiency in cerebellum. Structural covariance may reflect synchronized changes across regions. Part of these observations were similar to functional network, yet diverge from the results of structural network based on WM. Previously, a functional network study [35] reported decreased Eloc, Cp and increased Eg in patients with frontal LGGs, which were consistent with the results of ipsilesional unaffected regions network in our study. However, no alterations in small-world properties and Eg was observed in glioma patients based on a diffusion tensor imaging (DTI) study [34]. Partially overlapping observations between SCN and functional networks could arise from activity-dependent GM plasticity, as prior work shows partial concordance between structural covariance and resting-state functional networks in healthy adults [36]. Conversely, structural covariance does not directly map to anatomical connectivity. The divergence from WM networks underscores that structural covariance reorganization is not constrained

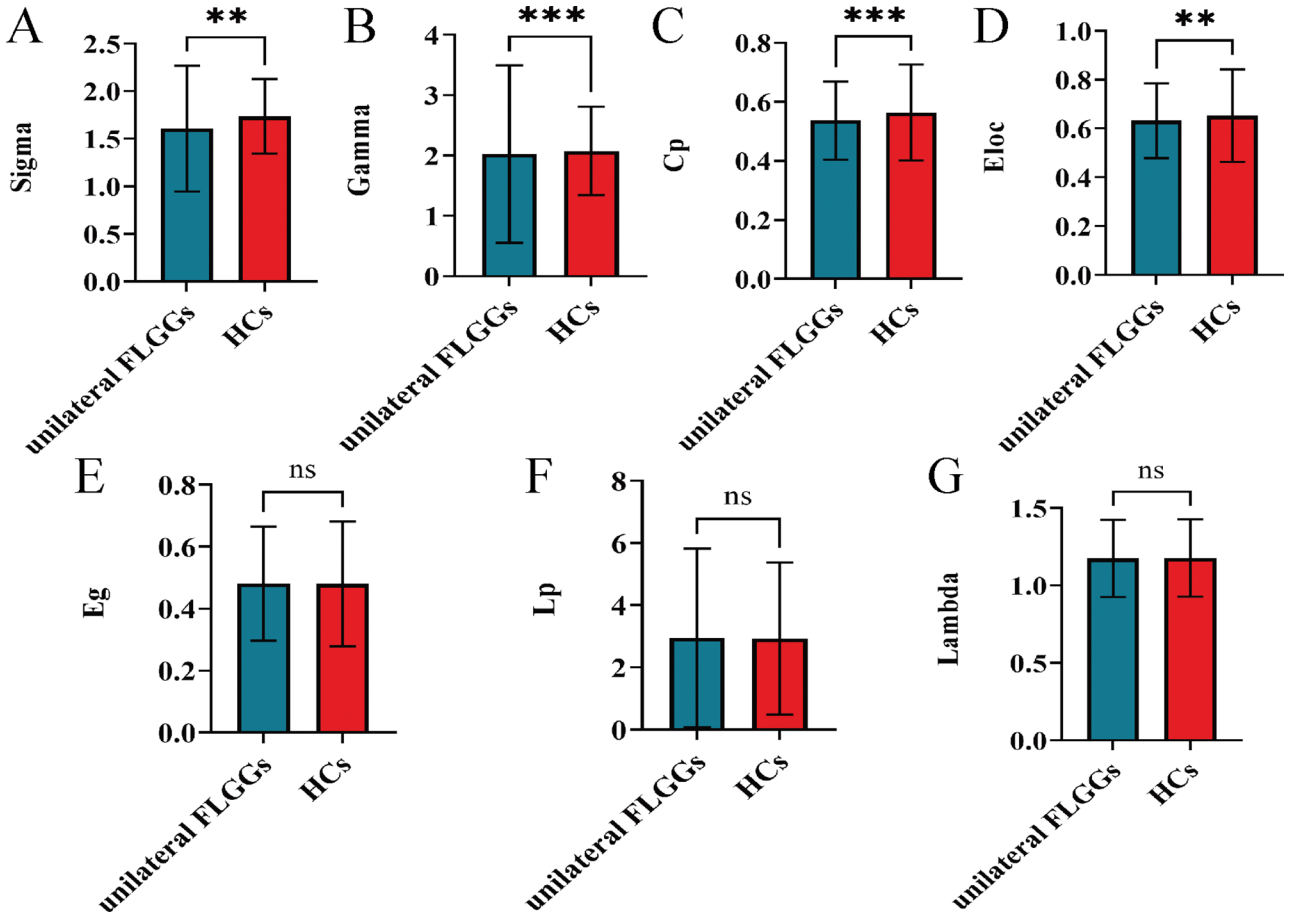

Fig. 8 Alterations in global network metrics of the cerebellum. Patients with unilateral FLGGs showed significantly decreased Sigma (**A**), Gamma (**B**), Cp (**C**) and Eloc (**D**) compared to HCs. Eg (**E**), Lp (**F**) and Lambda (**G**) did not differ significantly between groups. Sigma, small-world-ness; Gamma, normalized clustering coefficient; Lambda, normalized characteristic path length; Eg, global efficiency; Lp, characteristic path length; Eloc, local efficiency; Cp, clustering coefficient. FLGGs frontal lobe low-grade gliomas, HCs healthy controls

by direct anatomical tracts, potentially reflecting indirect or trans-synaptic mechanisms. These modality-specific findings collectively suggest glioma-induced neuroadaptation operates at multiple levels (morphological, structural, and functional) and each offer complementary insights.

The last key finding of our study was that nodal network metrics of several brain lobe and subcortical structures were changed significantly in unilateral FLGGs patients. In general, the distribution and changes of nodes were manifested as redistribution in the contralesional homologous structures, increases in the contralesional distal regions and decreases in the ipsilesional distal regions. BC quantifies the impact of a node on information flow within the network. DC assesses the connectivity of a node with other nodes in a network. NE measures the capacity for information propagation between a given node and other nodes. Our previous study on functional imaging found increased nodal network metrics in the remote areas of the lesion and decreased nodal network metrics in the lesion and its adjacent areas, which is not entirely consistent with our present results [32]. This discrepancy may be related to the non-synchronous alterations of functional and structural network.

Despite presenting novel findings, this study also has some limitations. First, the cohort of patients with right FLGGs was small. To enhance statistical power, we flipped patients with right-sided lesions to the left in our analysis. This operation could introduce bias due to the asymmetry between the left and right hemispheres. Therefore, the results of this study require further validation based on larger sample size and subgroup analysis. Second, the unaffected area referred to regions macroscopically free of tumor invasion on preoperative MRI in our study, but microscopic infiltration remains possible. More accurate pathological localization is needed to validate these results in the future. Last, this study did not integrate functional imaging and cognitive or behavioral assessments, which hindered to further explore the interaction between structure and function directly. Given that most patients in our study did not exhibit functional impairments, we speculate that these macrostructural

deviations may reflect neuroadaptation accumulated over years of indolent tumor growth. Future studies are needed to determine whether specific network changes correlate with clinical outcomes. Our cross-sectional study cannot directly establish causality or dynamic reorganization processes, as longitudinal designs are better suited to track neuroplastic changes over time. We will continue to collect longitudinal data for the study of dynamic glioma-induced neuroplasticity.

Conclusion

The combination of VBM and SCN analysis revealed both focal GMV enlargement and topological alterations in patients with unilateral FLGGs, and provide a novel perspective of cross regional morphological collaborative changes for understanding the glioma-related neuroadaptation. These findings may suggest potential neuroimaging correlates of adaptive changes, which could inform future investigations into personalized treatment approaches.

Abbreviations

3D	Three dimensional
AAL	Automated anatomical labeling
CNS	Central nervous system
CSF	Cerebrospinal fuid
DTI	Diffusion tensor imaging
FDR	false discovery rate
FLAIR	Fluid attenuation inversion recovery
FLGGs	Frontal lobe low-grade gliomas
FOV	Field of view
FWE	Family wise error
GM	Gray matter
GMV	Gray matter volume
HCs	Healthy controls
HGGs	High-grade gliomas
IDH	Isocitrate dehydrogenase
LGGs	Low-grade gliomas
MNI	Montreal neurological institute
MRI	Magnetic resonance imaging
SCN	Structural covariant network
SPSS	Statistical Package for the Social Sciences
TE	Echo time
TIV	Total intracranial volume
TR	Repetition time
TV	Tumor volume
VBM	Voxel-based morphometry
WM	White matter

Acknowledgements

None.

Author contributions

DYG and KL contributed to the study conception and design. Material preparation were performed by JX. Data collection and analysis, the draft of the manuscript and visualization were performed by YH and JXX. All authors read and approved the final manuscript.

Funding

This work was supported by the National Natural Science Foundation of China [grant numbers 82372048], Research Startup Fund of Huashan Hospital, Fudan University [grant numbers 2021QD035], Shanghai Sailing Program [grant numbers 22YF1405000], Shanghai Municipal Commission of Science and Technology [grant numbers 22TS1400900, 23S31904100, 22ZR1409500 and 22S31905300], Greater Bay Area Institute of Precision Medicine (Guangzhou) [grant numbers KCH2310094], and Science and Technology Commission of Shanghai Municipality [grant numbers 24SF1904200, 24SF1904201].

Data availability

The anonymized imaging database can be obtained after the reasonable request is evaluated and approved by the Ethics Committee of Huashan hospital, Fudan University. The data and materials of this study are available from the corresponding author on reasonable request.

Declarations

Ethics approval and consent to participate

All procedures performed in the studies involving human participants were in accordance with the ethical standards of the institutional and/or national research committee and with the 1964 Helsinki Declaration and its later amendments or comparable ethical standards. Informed consent was obtained from all individual participants included in the study. This study was approved by the institutional review board of Huashan Hospital, Fudan University.

Consent for publication

All authors agreed to publish all the contents of this study.

Competing interests

The authors declare no competing interests.

Received: 10 February 2025 / Accepted: 7 May 2025
Published online: 14 May 2025

References

1. Davis ME. Epidemiology and overview of gliomas. SEMIN ONCOL NURS. 2018;34(5):420–9. https://doi.org/10.1016/j.soncn.2018.10.001.
2. Draganski B, Gaser C, Busch V, et al. Neuroplasticity: changes in grey matter induced by training. Nature. 2004;427(6972):311–2. https://doi.org/10.1038/427311a.
3. Ismail FY, Fatemi A, Johnston MV. Cerebral plasticity: windows of opportunity in the developing brain. Eur J Paedatr Neuro. 2016;21(1):23–48. https://doi.org/10.1016/j.ejpn.2016.07.007.
4. Small SL, Hlustik P, Noll DC, et al. Cerebellar hemispheric activation ipsilateral to the Paretic hand correlates with functional recovery after stroke. Brain. 2002;125(Pt 7):1544–57. https://doi.org/10.1093/brain/awf148.
5. Siponkoski ST, Martínez-Molina N, Kuusela L, et al. Music therapy enhances executive functions and prefrontal structural neuroplasticity after traumatic brain injury: evidence from a randomized controlled trial. J NEUROTRAUM. 2019;37(4):618–34. https://doi.org/10.1089/neu.2019.6413.
6. Cargnelutti E, Ius T, Skrap M, et al. What do we know about pre- and post-operative plasticity in patients with glioma? A review of neuroimaging and intraoperative mapping studies. Neuroimage Clin. 2020;28:102435. https://doi.org/10.1016/j.nicl.2020.102435.
7. Huang Z, Li G, Li Z, et al. Contralesional structural plasticity in different molecular pathologic subtypes of insular glioma. Front Neurol. 2021;12(636573). https://doi.org/10.3389/fneur.2021.636573.
8. Krings T, Töpper R, Willmes K, et al. Activation in primary and secondary motor areas in patients with CNS neoplasms and weakness. Neurology. 2002;58(3):381–90. https://doi.org/10.1212/wnl.58.3.381.
9. Majos A, Bryszewski B, Kośla KN, et al. Process of the functional reorganization of the cortical centers for movement in GBM patients: fMRI study. Clin Neuroradiol. 2015;27(1):71–9. https://doi.org/10.1007/s00062-015-0398-7.
10. Lv K, Cao X, Wang R, et al. Contralesional macrostructural plasticity in patients with frontal low-grade glioma: a voxel-based morphometry study. Neuroradiology. 2022;65(2):297–305. https://doi.org/10.1007/s00234-022-03059-9.
11. Almairac F, Duffau H, Herbet G. Contralesional macrostructural plasticity of the insular cortex in patients with glioma: A VBM study. Neurology. 2018;91(20):e1902–8. https://doi.org/10.1212/WNL.0000000000006517.
12. Alexander-Bloch A, Giedd JN, Bullmore E. Imaging structural co-variance between human brain regions. Nat Rev Neurosci. 2013;14(5):322–36. https://doi.org/10.1038/nrn3465.
13. Blumen HM, Allali G, Beauchet O, et al. A Gray matter volume covariance network associated with the motoric cognitive risk syndrome: A multicohort

MRI study. J Gerontol A Biol. 2019;74(6):884–9. https://doi.org/10.1093/gerona/gly158.
14. Lee PL, Chou KH, Lu CH, et al. Extraction of large-scale structural covariance networks from grey matter volume for Parkinson's disease classification. Eur Radiol. 2018;28(8):3296–305. https://doi.org/10.1007/s00330-018-5342-1.
15. Chang YT, Huang CW, Chang WN et al. Altered Functional Network Affects Amyloid and Structural Covariance in Alzheimer's Disease. Biomed Res Int. 2018; 2018 8565620. https://doi.org/10.1155/2018/8565620
16. Louis DN, Perry A, Wesseling P, et al. The 2021 WHO classification of tumors of the central nervous system: a summary. Neurooncology. 2021;23(8):1231–51. https://doi.org/10.1093/neuonc/noab106.
17. Benarroch EE. The amygdala: functional organization and involvement in neurologic disorders. Neurology. 2014;84(3):313–24. https://doi.org/10.1212/WNL.0000000000001171.
18. Ray D, Hajare N, Roy D, et al. Large-scale functional integration, rather than functional dissociation along dorsal and ventral streams, underlies visual perception and action. J Cogn Neurosci. 2020;32(5):847–61. https://doi.org/10.1162/jocn_a_01527.
19. Sereno MI, Dale AM, Reppas JB, et al. Borders of multiple visual areas in humans revealed by functional magnetic resonance imaging. Science. 1995;268(5212):889–93. https://doi.org/10.1126/science.7754376.
20. Kuhnke P, Chapman CA, Cheung VKM, et al. The role of the angular gyrus in semantic cognition: a synthesis of five functional neuroimaging studies. Brain Struct Funct. 2022;228(1):273–91. https://doi.org/10.1007/s00429-022-02493-y.
21. Humphreys GF, Lambon Ralph MA, Simons JSA. Unifying account of angular gyrus contributions to episodic and semantic cognition. Trends Neurosci. 2021;44(6):452–63. https://doi.org/10.1016/j.tins.2021.01.006.
22. Davey J, Cornelissen PL, Thompson HE, et al. Automatic and controlled semantic retrieval: TMS reveals distinct contributions of posterior middle Temporal gyrus and angular gyrus. J Neurosci. 2015;35(46):15230–9. https://doi.org/10.1523/JNEUROSCI.4705-14.2015.
23. Xu J, Elazab A, Liang J, et al. Cortical and subcortical structural plasticity associated with the glioma volumes in patients with cerebral gliomas revealed by Surface-Based morphometry. Front Neurol. 2017;8:266. https://doi.org/10.3389/fneur.2017.00266.
24. Liu Y, Hu G, Yu Y, et al. Structural and functional reorganization within cognitive control network associated with protection of executive function in patients with unilateral frontal gliomas. Front Oncol. 2020;10:794. https://doi.org/10.3389/fonc.2020.00794.
25. Zhang G, Zhang X, Huang H, et al. Probing individual-level structural atrophy in frontal glioma patients. Neurosurg Rev. 2022;45(4):2845–55. https://doi.org/10.1007/s10143-022-01800-9.
26. Timmann D, Drepper J, Frings M, et al. The human cerebellum contributes to motor, emotional and cognitive associative learning. A review. Cortex. 2009;46(7):845–57. https://doi.org/10.1016/j.cortex.2009.06.009.
27. Marvel CL, Desmond JE. The contributions of cerebro-cerebellar circuitry to executive verbal working memory. Cortex. 2009;46(7):880–95. https://doi.org/10.1016/j.cortex.2009.08.017.
28. Murdoch BE. The cerebellum and Language: historical perspective and review. Cortex. 2009;46(7):858–68. https://doi.org/10.1016/j.cortex.2009.07.018.
29. Starowicz-Filip A, Chrobak AA, Kwiatkowski S, et al. Cerebellar lesions after low-grade tumor resection can induce memory impairment in children, similar to that observed in patients with frontal lesions. Child Neuropsychol. 2019;26(3):388–408. https://doi.org/10.1080/09297049.2019.1657391.
30. Deviaterikova A, Kasatkin V, Malykh S. The role of the cerebellum in Visual-Spatial memory in pediatric posterior Fossa tumor survivors. Cerebellum. 2023;23(1):197–203. https://doi.org/10.1007/s12311-023-01525-5.
31. Zhang N, Xia M, Qiu T, et al. Reorganization of cerebro-cerebellar circuit in patients with left hemispheric gliomas involving Language network: A combined structural and resting-state functional MRI study. Hum Brain Mapp. 2018;39(12):4802–19. https://doi.org/10.1002/hbm.24324.
32. Lv K, Hu Y, Cao X, et al. Altered whole-brain functional network in patients with frontal low-grade gliomas: a resting-state functional MRI study. Neuroradiology. 2024;66(5):775–84. https://doi.org/10.1007/s00234-024-03300-7.
33. Park JE, Kim HS, Kim SJ, et al. Alteration of long-distance functional connectivity and network topology in patients with supratentorial gliomas. Neuroradiology. 2015;58(3):311–20. https://doi.org/10.1007/s00234-015-1621-6.
34. Liu Y, Yang K, Hu X, et al. Altered Rich-Club organization and regional topology are associated with cognitive decline in patients with frontal and Temporal gliomas. Front Hum Neurosci. 2020;14(23). https://doi.org/10.3389/fnhum.2020.00023.
35. Huang Q, Zhang R, Hu X, et al. Disturbed small-world networks and neurocognitive function in frontal lobe low-grade glioma patients. PLoS ONE. 2014;9(4):e94095. https://doi.org/10.1371/journal.pone.0094095.
36. Hosseini SM, Kesler SR. Comparing connectivity pattern and small-world organization between structural correlation and resting-state networks in healthy adults. NeuroImage. 2013;78:402–14. https://doi.org/10.1016/j.neuroimage.2013.04.032.

Publisher's note

Springer Nature remains neutral with regard to jurisdictional claims in published maps and institutional affiliations.